Seismic Retrofit of Low-Rise Reinforced-Concrete Buildings: A Modified Displacement-Based Design Procedure

Adriano De Sortis, Ph.D.[1]; and Fabrizio Vestroni[2]

Abstract: A noniterative procedure to determine the retrofitted configuration of an existing building, to be assessed according to the seismic code, is proposed. Among possible rehabilitation strategies, the approach involving both stiffness and strength increments has been followed, maintaining yielding and ultimate displacements unchanged. Limiting our focus to low-rise reinforced-concrete buildings, under the hypotheses of shear-type behavior and constant axial forces in the columns, the yielding and ultimate displacements of a single-degree-of-freedom (SDOF) system, equivalent to the existing multi-degree-of-freedom (MDOF) system, are determined. Using the SDOF displacement capacity, the displacement design spectrum furnishes the corresponding period and, then, the required stiffness and strength are determined. Hence, returning to the MDOF system, the demand at each floor in terms of shear resistance can be assessed. The difference between required and available shear resistances is provided by additional elements, in this case steel bracings are adopted. The discussion of a case study clarifies the various steps described, also confirming the suitability of the assumptions introduced, with special attention paid to the vertical regularity of the whole structure or of the added elements alone. Moreover, nonlinear dynamic responses to a set of natural accelerograms are used to evaluate the effectiveness of the proposed approximate design procedure. **DOI: 10.1061/(ASCE)AE.1943-5568.0000398**.

Author keywords: Seismic retrofit; Existing buildings; Displacement-based design; Reinforced concrete; Low-rise buildings; Steel bracings; Nonlinear dynamic analysis.

Introduction

The first step of the retrofit design of existing buildings is the evaluation of their seismic performance. To this aim, recourse is usually made to the nonlinear static analysis procedure, widely applied for the seismic assessment in international seismic codes and standards (ASCE 2013; FEMA 2005; ATC 1996), as in the Italian seismic Code (NTC 2018). The pertinent part of this code is mainly based on Annex B of EN 1998-1 (2004) and Annex A of EN 1998-3 (2005), that, in turn, follows the method proposed in Fajfar (1999) and Fajfar and Gašperšič (1996).

The displacement-based design, proposed in Qi and Moehle (1991) and Moehle (1992) more than two decades ago for new buildings subjected to seismic actions, is a rational design tool in which the control of the period of the structure becomes an effective design procedure. The approach developed in Qi and Moehle (1991) and Moehle (1992) was based on the use of conventional 5% damping response spectra and initial stiffness of the structure. Approaches based on ultimate secant stiffness and equivalent damping, depending on available ductility and structure typology, have been developed in Priestley (1993) and Medhekar and Kennedy (2000). According to the investigations reported in Chopra and Goel (2001) and Miranda and Ruiz-Garcia (2002) there is no clear evidence that methods based on secant stiffness produce better estimates of inelastic displacement demands.

The capabilities of displacement-based procedures for the design of new buildings have been explored by several researchers (Sullivan et al. 2003; Vidot-Vega and Kowalsky 2013; Panagiotakos and Fardis 2001), and their effectiveness has been thoroughly proved; in particular, it has been shown that interstory drifts for the frames designed using this approach correlated well with the values obtained from large sets of numerical simulations.

For the existing buildings, if the seismic assessment is not satisfied, a retrofit strategy must be pursued. In Chapter 1 of ASCE (2013), as in other codes, different retrofit strategies are discussed from a qualitative point of view. In practice, several tentative retrofit configurations are usually analyzed until the performance required by seismic codes is achieved. Once the strategy has been selected, the displacement-based procedures can be followed; its use for existing buildings has been already investigated in the literature (Priestley 1997; Grande and Rasulo 2013), mainly dealing with specific cases and leaving some issues still open, as highlighted in the following. Some papers are focused on dissipative devices (Kim and Choi 2006; Lin et al. 2008; Barbagallo et al. 2018; Nuzzo et al. 2019), some on steel structures or on peculiar typologies (Grande and Rasulo 2015; Rossi 2007; Sun et al. 2018), in some of them the modification of the deflected shape of the structure or the elimination of torsional coupling of modal shapes are enforced (Thermou et al. 2007; Thermou and Psaltakis 2018).

The present paper places itself among the studies based on displacement-based procedures for the seismic assessment of existing buildings, focusing attention on a straightforward procedure to directly determine the retrofitted configuration of the building, instead of the usual trial-and-error path. With respect to previous contributions the simple use of ordinary bracings has been referred to, maintaining the original deflected shape and torsional coupling of the existing structure, in order to minimize the impact of the intervention. Furthermore, when adding new structural elements to the

[1]Structural Engineer, Dept. of Civil Protection, Via Vitorchiano 2, 00189 Rome, Italy (corresponding author). ORCID: https://orcid.org/0000-0002-3387-8261. Email: adriano.desortis@protezionecivile.it

[2]Professor, Dept. of Structural and Geotechnical Engineering, Sapienza University of Rome, Via Eudossiana 18, 00184 Rome, Italy. Email: vestroni@uniroma1.it

Note. This manuscript was submitted on November 27, 2018; approved on October 18, 2019; published online on March 30, 2020. Discussion period open until August 31, 2020; separate discussions must be submitted for individual papers. This paper is part of the ***Journal of Architectural Engineering***, © ASCE, ISSN 1076-0431.

existing structure, special attention has been paid to avoiding vertical irregularity due both to the existing structure and to the additional system, an aspect not explicitly addressed previously in the literature.

After a discussion in "Rehabilitation Strategies", a modified displacement-based approach is proposed in "Design of the Retrofitted Structural Configuration". Here this approach is adjusted, in order to be applied to existing structures: starting from knowledge of the displacement capacity of a substitute SDOF system, equivalent to the existing MDOF, the corresponding vibration period obtained from the displacement response spectrum becomes the target of the structure, which is obtained through a suitable increase of strength and stiffness of the structure by adding new elements. Focusing on low-rise reinforced concrete buildings, the hypotheses of shear-type behavior and constant axial member forces, usually valid for those buildings, allow us to achieve the retrofitted configuration in closed form. In "Case Study," the procedure is applied to a real case, in the framework of a seismic retrofit project of a strategic building in L'Aquila, Italy, where additional steel bracings are used for retrofitting purposes. The case study permitted us to verify the applicability of the proposed approach and to discuss the effectiveness of the procedure on the basis of a dynamic nonlinear analysis, summarizing the main outcomes of the work in "Conclusions".

Rehabilitation Strategies

Prior to performing the design of the rehabilitation interventions, an assessment of the existing structure is needed. As referred to in the "Introduction," nonlinear static analysis is widely adopted in modern seismic codes. Thus, this tool, as reported in NTC (2018), is suitable for investigating different rehabilitation strategies.

Reinforced concrete buildings are considered here. The structure, modeled as a multi-degree-of-freedom (MDOF) system, is subjected to a path of horizontal loads scaled with one parameter, the load multiplier. The horizontal displacement of one point, usually located at the roof level, is controlled during the analysis, until the displacement capacity of some elements is reached or a global resistance drop of more than 15% is observed. The corresponding displacement is assumed as the displacement capacity, if no fragile collapse mechanisms is activated previously. Otherwise, the displacement capacity must be reduced accordingly.

The relationship of the load multiplier versus control point displacement (pushover curve) allows us to define a single-degree-of-freedom (SDOF) substitute structure, having a bilinear force–displacement constitutive law. Thus, the mass M^*, the initial stiffness K^*, the elastic period $T^* = 2\pi\sqrt{M^*/K^*}$, the strength R_y^*, the yielding displacement D_y^*, and the displacement capacity D_u^* of the equivalent SDOF system are obtained. Knowing T^*, the displacement demand $D_{\max}^*$ to the SDOF substitute structure is estimated using the design 5% damping displacement spectrum depicted in Fig. 1(a), where the design acceleration response spectrum is also reported.

Points 1, 2, and 3 on the design response spectrum [Fig. 1(a)] correspond to three different ranges ($T^* > T_C$, $T_B < T^* < T_C$, and $T^* < T_B$, respectively). The conventional response spectra parameters (including T_B and T_C) are defined by the seismic code for the limit state of interest (usually life safety or collapse prevention). In Range 1, the inelastic displacement demand $D_{\max,1}^*$ coincides with the maximum displacement $S_{De}(T^* = T_1^*)$ of an elastic SDOF system having the same period T_1^*

$$D_{\max,1}^* = S_{De}(T_1^*) = S_{ae}(T_1^*)\frac{T_1^{*2}}{4\pi^2} \tag{1}$$

where $S_{ae}(T_1^*)$ = the acceleration spectral ordinate. In Range 2, according to NTC (2018) and Fajfar (1999), the inelastic displacement

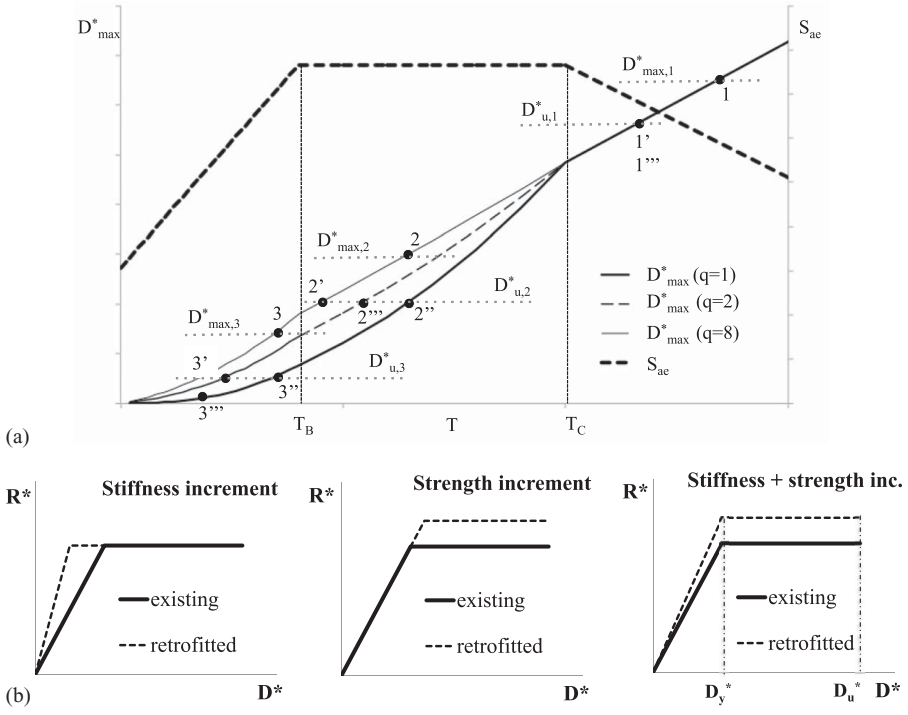

Fig. 1 (a) Acceleration and displacement design response spectra according to NTC (2018) (q^* is the ratio between the maximum restoring force on an elastic system having the same period and the restoring force at yielding); and (b) rehabilitation strategies on a SDOF system with stiffness increment, strength increment, and both stiffness and strength increments.

J. Archit. Eng., 2020, 26(2): 04020008

demand $D^*_{\max,2}$ is greater than $S_{De}(T^* = T^*_2)$

$$D^*_{\max,2} = \frac{1 + (q^* - 1)T_C/T^*_2}{q^*} S_{De}(T^*_2) \quad (2)$$

where

$$q^* = \frac{M^* S_{ae}(T^*_2)}{R^*_y} \quad (3)$$

is the ratio between the maximum response force on an elastic SDOF having the same period T^*_2 and the substitute SDOF force at yielding. In Range 3, the same expressions (2) and (3) must be adopted, changing T^*_2 with T^*_3.

If the displacement demand $D^*_{\max}$ is greater than the displacement capacity D^*_u, a rehabilitation intervention is necessary. An increment of D^*_u appears to be the most natural strategy, but in many cases this is not convenient, especially when large numbers of elements are involved.

Thus, assuming that D^*_u remains unchanged after the interventions, different retrofit strategies can be explored [Fig. 1(b)]: stiffness increment, strength increment, and both stiffness and strength increments. If only the stiffness is increased, yielding displacement D^*_y decreases (required ductility increases); if the increment concerns only the strength, yielding displacement increases (required ductility decreases); in the third strategy it is assumed here that the yielding displacement is unchanged (same ductility).

Interventions based on composite materials substantially resemble the second strategy (increment of strength without significant increment of stiffness). Interventions based on additional ductile elements for the absorption of the horizontal actions resemble the third strategy (a stiffness increment usually involves a strength increment). If the additional elements for the absorption of the horizontal actions exhibit a fragile behavior (such as hollow clay masonry infills) the intervention substantially belongs to the first strategy.

In order to move the SDOF status from Point 1 to Points 1′ or 1‴ (reduction of $D^*_{\max,1}$), both strategies involving a stiffness increment are able to reduce the period and are effective in pursuing the goal, whereas the second strategy is not effective. For Point 2, the goal can be obtained with a stiffness increment (Point 2′), a strength increment (Point 2″), or both (Point 2‴). For Point 3, a stiffness increment (Point 3′) also implies a reduction of q^* (S_{ae} decreases); an increment of strength (Point 3″) and of both (Point 3‴) complete the possible choices among retrofit strategies.

In the case study dealt with in the following, the retrofit is obtained using additional ductile elements, which corresponds to the third strategy.

Design of the Retrofitted Structural Configuration

The seismic retrofit design generally starts with the nonlinear static or dynamic analyses of the existing structure. Then, an iterative approach is usually applied, in which several modifications of the original configuration are analyzed, until the performance required by the considered limit state is achieved.

In this section, a procedure is proposed that, under reasonable assumptions, leads directly to the definition of the retrofitted configuration, which will be verified according to the seismic code.

The original formulation developed by Moehle (1992) for the design of new buildings has been modified for existing buildings. As already discussed in the "Introduction," in several papers, approaches based on ultimate secant stiffness and overdamped response spectra are becoming more popular. Here, the approach based on the initial stiffness and 5% damped response spectrum is felt to be more suitable, because of its compatibility with codified analysis procedures.

Some of the following expressions are well known, nevertheless they are reported to facilitate the description of the methodology. The discussion is initially devoted to a SDOF system, and then extended to a MDOF system. For an existing SDOF system, yielding displacement D^*_y, ultimate displacement D^*_u, and available ductility $\mu^* = D^*_u/D^*_y$ are known. According to the strategy based on both stiffness and strength increments in Fig. 1(b), D^*_y and D^*_u remain unchanged between original and retrofitted configurations. Thus, to satisfy the performance, $D^*_{\max} \le D^*_u$. If D^*_u falls in Range 1 of Fig. 1(a), the value of $T^* = T^*_1$ can be obtained directly by inverting Eq. (1) and the initial stiffness of the SDOF system can be calculated

$$K^* = \frac{4\pi^2 M^*}{T^{*2}} \quad (4)$$

The required strength of the SDOF system is

$$R^*_y = K^* D^*_y \quad (5)$$

If the available strength is smaller than that evaluated with Eq. (5), the strength must be increased through a retrofit intervention.

If D^*_u falls in Range 2, Fig. 1(a), the value of q^* to be put in Eq. (2) must be known; to this aim, an initial guess of $T^* = T^*_2$ is made with $q^* = \mu^*$. The period T^*_2, the stiffness [Eq. (4)] and the strength [Eq. (5)] can be obtained and the value of $S_{ae}(T^*_2)$ is determined; a new guess of q^* is obtained applying Eq. (3), leading to the correct value. The same holds if D^*_u falls in Range 3 [Fig. 1(a)].

When dealing with a MDOF system, a substitute SDOF system with similar overall characteristics is introduced. The dimensionless equation of motion of a SDOF system, having an elastic–perfectly plastic bilinear force–displacement law, can be written as

$$\ddot{\mu}(t) + 2\xi\omega\dot{\mu}(t) + \omega^2\rho(t) = -\frac{\omega^2}{\eta}\frac{\ddot{u}_g(t)}{\ddot{u}_{g,\max}} \quad (6)$$

where $\mu(t) = u(t)/u_y$; $u(t)$ = the SDOF relative displacement with respect to the ground at time t; u_y = the displacement at yielding; $\rho(t) = r(t)/r_y$, $r(t)$ = the restoring force; r_y = the force at yielding; $\omega = \sqrt{r_y/(mu_y)}$ = the natural frequency in the elastic range; m = the mass of the system; ξ = the relative damping; $\eta = r_y/(m\ddot{u}_{g,\max})$, $\ddot{u}_g(t)$ = the ground acceleration; and $\ddot{u}_{g,\max}$ = the peak ground acceleration. For a MDOF system the motion equations are

$$\mathbf{M}\ddot{\mathbf{u}}(t) + \mathbf{C}\dot{\mathbf{u}}(t) + \mathbf{R}(t) = -\mathbf{M}\mathbf{I}\ddot{u}_g(t) \quad (7)$$

where $\mathbf{u}$ = the displacement vector; $\mathbf{M}$ = the mass matrix; $\mathbf{C}$ = the damping matrix; $\mathbf{R}$ = the nodal forces vector; and $\mathbf{I}$ = the identity column vector. The following constraint allows to separate the spatial variability from the time variability:

$$\mathbf{u}(t) \simeq \mathbf{s}D^*(t) \quad (8)$$

where $D^*(t)$ = the displacement of a reference point; and $\mathbf{s}$ = a suitable shape vector. This shape represents the desired deflected shape of the retrofitted building. By replacing Eq. (8) in Eq. (7) and premultiplying by $\mathbf{s}^T$ we obtain

$$M^*\ddot{D}^*(t) + C^*\dot{D}^*(t) + R^*(t) = -L^*\ddot{u}_g(t) \quad (9)$$

where $M^* = \mathbf{s}^T\mathbf{M}\mathbf{s}$; $C^* = \mathbf{s}^T\mathbf{C}\mathbf{s}$; $L^* = \mathbf{s}^T\mathbf{M}\mathbf{I}$; and $R^*(t) = \mathbf{s}^T\mathbf{R}(t)$. The following parameters can be defined: $K^* = R^*_y/D^*_y$, $\omega^{*2} = K^*/M^*$,

$2\xi\omega^* = C^*/M^*$, $\rho^*(t) = R^*(t)/R_y^*$, $\mu^*(t) = D^*(t)/D_y^*$, and $\eta^* = R_y^*/(M^*\ddot{u}_{g,\max})$. The parameters R_y^* and D_y^* correspond to the conventional yielding point of the equivalent system. After the previous definitions, Eq. (9) becomes

$$\ddot{\mu}^*(t) + 2\xi\omega^*\dot{\mu}^*(t) + \omega^{*2}\rho^*(t) = -\frac{L^*}{M^*}\frac{\omega^{*2}}{\eta^*}\frac{\ddot{u}_g(t)}{\ddot{u}_{g,\max}} \tag{10}$$

By comparing Eqs. (6) and (10), it is evident that the response of the substitute SDOF system can be obtained multiplying by L^*/M^* the response of a SDOF system characterized by the parameters reported previously.

In order to characterize the bilinear force–displacement relation, the deflected shape at yielding is assumed as a shape vector. This shape vector depends only on the characteristics of the existing elements, owing to the assumption that both D_y^* and D_u^* remain unchanged between the original and retrofitted configuration. The following constraints allow the evaluation of the deflected shape: (i) the variation of the axial force on the column is neglected (the values of axial forces under vertical loads are assumed); (ii) the seismic behavior is shear type (this implies that the joint rotations coincide with the chord rotations of the vertical elements and that the beams behave elastically). For each principal direction of the building plan, for each level and for each vertical element the corresponding yielding chord rotation can be calculated using expressions from the literature; here the formulation reported in NTC (2018) is adopted. A unique representative value for yielding chord rotations $\theta_{y,i}$ of the vertical elements at Level i is assumed. Usually, the mean value among all elements is a reasonable choice. If a significant building torsion is expected, the approach described in Paulay (1997) should be applied, with expressions governed by the overall strength and by the stiffness eccentricity. At this point of the design procedure, the positions and characteristics of the additional bracings are not yet known. It is reasonable to assume that the presence of the additional elements should reduce the building torsion of the retrofitted structure, thus the aforementioned approach can be safely applied by considering only the elements of the existing structure.

The relative displacements between the floors are $\delta_{y,i} = \theta_{y,i}H_i$, where H_i is the height of the ith interstory. The corresponding displacements of the jth floor result in

$$d_{y,j} = \sum_{i=1}^{j}\delta_{y,i} \tag{11}$$

At yielding, it is assumed $u_j = d_{y,j}$, and from Eq. (8) the corresponding components of the shape vector are obtained by

$$s_j = d_{y,j}/D_y^* \tag{12}$$

The displacement D_y^* can be calculated by recalling that $M^* = \mathbf{s}^T\mathbf{M}\mathbf{s}$ and imposing that the equivalent SDOF system had the same mass of the structure, $M^* = \sum_{i=1}^{N} m_i$

$$D_y^* = \sqrt{\frac{\sum_{i=1}^{N} m_i d_{y,i}^2}{\sum_{i=1}^{N} m_i}} \tag{13}$$

The factor L^*/M^* results in

$$\frac{L^*}{M^*} = \frac{1}{D_y^*}\frac{\sum_{i=1}^{N} m_i d_{y,i}}{\sum_{i=1}^{N} m_i} \tag{14}$$

Similarly, at ultimate conditions, the chord rotations $\theta_{u,i}$ of the vertical elements at Level i can be estimated. In this case, the selection of the minimum value among all elements is a reasonable choice. If a significant building torsion is expected, the approach already recalled for the yielding condition should be applied. The relative displacements between the floors is $\delta_{u,i} = \theta_{u,i}H_i$. The corresponding displacements of the jth floor result in

$$d_{u,j} = \sum_{i=1}^{j}\delta_{u,i} \tag{15}$$

The available ductility μ^* is assumed as the minimum value of the ratios $d_{u,j}/d_{y,j}$ at each floor. The ultimate SDOF equivalent displacement is thus

$$D_u^* = \mu^* D_y^* \tag{16}$$

At this point, the period T^* can be calculated from Eq. (1) or Eqs. (2) and (3), substituting $M^*D_u^*/L^*$ and $M^*D_y^*/L^*$ to $D_{\max}^*$ and D_y^* respectively, and then Eqs. (4) and (5) can be applied, obtaining R_y^*. Recalling Eq. (12) and considering that

$$R_y^* = K^*D_y^* = \mathbf{s}^T\mathbf{R} = \frac{\sum_{i=1}^{N} d_{y,i}R_i}{D_y^*} \tag{17}$$

Eq. (13) can be substituted into (17), finally obtaining

$$\sum_{i=1}^{N} d_{y,i}R_i = K^*D_y^{*2} = K^*\frac{\sum_{i=1}^{N} m_i d_{y,i}^2}{M^*} \tag{18}$$

At this point, the forces R_i must be determined in order to satisfy (18). One of the possible choices to satisfy Eq. (18) is to set that each term of the two summations must be equal, thus obtaining

$$R_i = \frac{m_i d_{y,i}}{M^*}K^* \tag{19}$$

Eq. (19) is usually applied during the design of new buildings. Often, when dealing with existing buildings, some constraints arising from the actual characteristics of the structure suggest a more flexible approach. Thus, a different solution is obtained if a condition on the regularity in elevation is introduced, as discussed in the following. Calling K_i the lateral stiffness of the ith level, the regularity condition corresponds to

$$K_i = \alpha K_{i+1} \tag{20}$$

According to NTC (2018), the parameter α is selected in the range [0.9–1.4]. Considering that the shear V_i acting at the ith level is

$$V_i = \sum_{k=i}^{N} R_k \tag{21}$$

the floor stiffness of the Nth level is

$$K_N = \frac{V_N}{\delta_{y,N}} = \frac{R_N}{\delta_{y,N}} \tag{22}$$

and R_N can be easily calculated as

$$R_N = K_N\delta_{y,N} \tag{23}$$

At Level $N-1$ the lateral stiffness is

$$K_{N-1} = \frac{V_{N-1}}{\delta_{y,N-1}} = \frac{R_N + R_{N-1}}{\delta_{y,N-1}} \tag{24}$$

J. Archit. Eng., 2020, 26(2): 04020008

and, considering Eq. (20), R_{N-1} results in

$$R_{N-1} = \alpha K_N \delta_{y,N-1} - R_N \tag{25}$$

Substituting the previous recursive expressions into Eq. (18), the stiffness K_N can be evaluated:

$$K_N = \frac{K^*}{M^*} \frac{\sum_{i=1}^{N} m_i d_{y,i}^2}{\sum_{i=1}^{N} \alpha^{N-i} \delta_{y,i} d_{y,i} - \sum_{i=1}^{N-1} \alpha^{N-i-1} \delta_{y,i+1} d_{y,i}} \tag{26}$$

The force R_N is given by Eq. (23), whereas the remaining forces R_i ($i = 1 \ldots N-1$) are determined with

$$R_i = \alpha^{N-i} K_N \delta_{y,i} - \sum_{k=i+1}^{N} R_k \tag{27}$$

This leads to a different distribution of lateral loads, with respect to the solution (19), satisfying the additional conditions (20) on the vertical regularity.

The total shear V_i required at Level i is evaluated with Eq. (21). Under the assumptions introduced, the available shear $V_{bldg,i}$ at Level i is obtained by summing the shear resistance of all the vertical elements. The characteristics of the additional elements can be calculated in order to gather the needed additional shear resistance $V_{add,i}$

$$V_{add,i} = V_i - V_{bldg,i} \tag{28}$$

When the solution leads to a retrofitted configuration with abrupt strength changes of the additional bracings, a different criterion could be more suitable, based on the elevation regularity of the additional bracings, corresponding to the constraint

$$V_{add,i} = \beta V_{add,i+1} \tag{29}$$

Applying a procedure similar to that discussed for the elevation regularity of the whole building, the shear resistance of the additional bracings at the Nth level results in

$$V_{add,N} = \frac{\frac{K^*}{M^*} \sum_{i=1}^{N} m_i d_{y,i}^2 - \sum_{i=1}^{N} V_{bldg,i} \delta_{y,i}}{d_{y,N} + \sum_{i=1}^{N-1} (\beta^{N-i} - \beta^{N-i-1}) d_{y,i}} \tag{30}$$

The force R_N is given by

$$R_N = V_N = V_{bldg,N} + V_{add,N} \tag{31}$$

and the other forces R_i ($i = 1 \cdots N-1$) are given by

$$R_i = V_{bldg,i} - V_{bldg,i+1} + (\beta^{N-i} - \beta^{N-i-1}) V_{add,N} \tag{32}$$

According to the strategy based on both stiffness and strength increments, the stiffness of the added elements must be selected in order to exhibit the same yielding displacement of the existing structure.

When the satisfaction of the operational limit state, such as the maximum interstory drift for strategic buildings, is required, it can be shown that this can be obtained by a scaling of the displacement demands estimated previously at each level.

Case Study

The building to be retrofitted [Figs. 2(a and b)] is part of a complex, housing the Abruzzo Regional Fire Service Department, L'Aquila. The building has two floors and a flat roof. The structural plans of the foundations and of the first floor slab are reported in Figs. 2(c and d). Each floor has a surface of about 600 m^2. The plan is L-shaped with dimensions of 32.4 and 25.8 m. The 30-cm thick slabs are made of precast elements, lightening blocks, and a cast-in-place reinforced concrete layer. The foundations consist of reverse beams. Three reinforced concrete, hollow-core walls house the stairs and the elevator. The columns are 40 cm in diameter circular and 30×30 or 30×50-cm^2 rectangular. In general, the rectangular columns are reinforced with four or six 16-mm diameter longitudinal bars and 6-mm diameter stirrups spaced 15 cm apart; the circular columns are reinforced with six 16-mm diameter longitudinal bars and 6-mm diameter stirrups spaced 15 cm apart. The internal beams have the same depth as the slabs, and the perimetric beams depth is 60 cm.

The building was designed in 1990 complying to a code based on allowable stress checks. It was designed taking into account the seismic loads and almost all the horizontal resistance was provided by the circular hollow core walls, whereas the rectangular hollow-core walls and the columns were designed only for the vertical loads.

It suffered minor damage during the recent 2009 earthquake. The good performance of the building can be partially attributed to the presence of masonry infill walls. The return period of the 2009 main event can be estimated to be about 600 years according to Price et al. (2012) and Cáelebi et al. (2010), whereas the retrofit project was intended for a seismic action of about 2,500 years. Thus, significant modifications of the structural layout of the building are expected to cope with this goal. The results in the global X direction [Fig. 2(c)] are discussed; similar conclusions have been obtained in the global Y direction.

According to the proposed procedure, the following assumptions were made: (i) the retrofit is based on the addition of new steel-braced frames [elements *br* in Fig. 2(d)], (ii) the axial forces in the vertical elements, owing to the dead and live loads, do not change under the seismic loads, and (iii) the behavior of the building is shear type. The suitability of these hypotheses are checked at the end with nonlinear dynamic simulations.

Before applying the design procedure, the occurrence of fragile collapses must be checked for each member, comparing the shear resistance with the shear force equilibrating the flexural strength. The shear resistance is assumed as the minimum shear carried by the concrete or by the reinforcements. These checks were satisfied for all the columns. The shear carried by the concrete is greater than that equilibrating the flexural strength only for the hollow rectangular elevator shaft. The remaining circular hollow-core walls are far from this requisite and upgrading of the concrete shear resistance was deemed unreliable. According to NTC (2018), the hollow circular walls cannot be considered as secondary elements, because they would carry more than 15% of the horizontal loads. Thus, they will be deactivated [elements *de* in Fig. 2(d)] to minimize their flexural stiffness and assure their capacity only against vertical loads.

For the hollow rectangular elevator shaft, the shear carried by the reinforcements is smaller than that equilibrating the flexural strength and requires an upgrade [element *st* in Fig. 2(d)]. Moreover, because the story diaphragms are assumed as rigid, new portions of slabs [*sl* in Fig. 2(d)] are added, to eliminate the weakness owing to the irregular shape of the floor slabs near the inner circular core.

The design procedure starts with the selection of the design yielding chord rotation at each floor. The details of the closed-form estimation of the chord rotations of each element are omitted, while synthetic values are reported in Table 1. At yielding, very similar mean values of 0.8%–0.9% at both levels can be observed for the

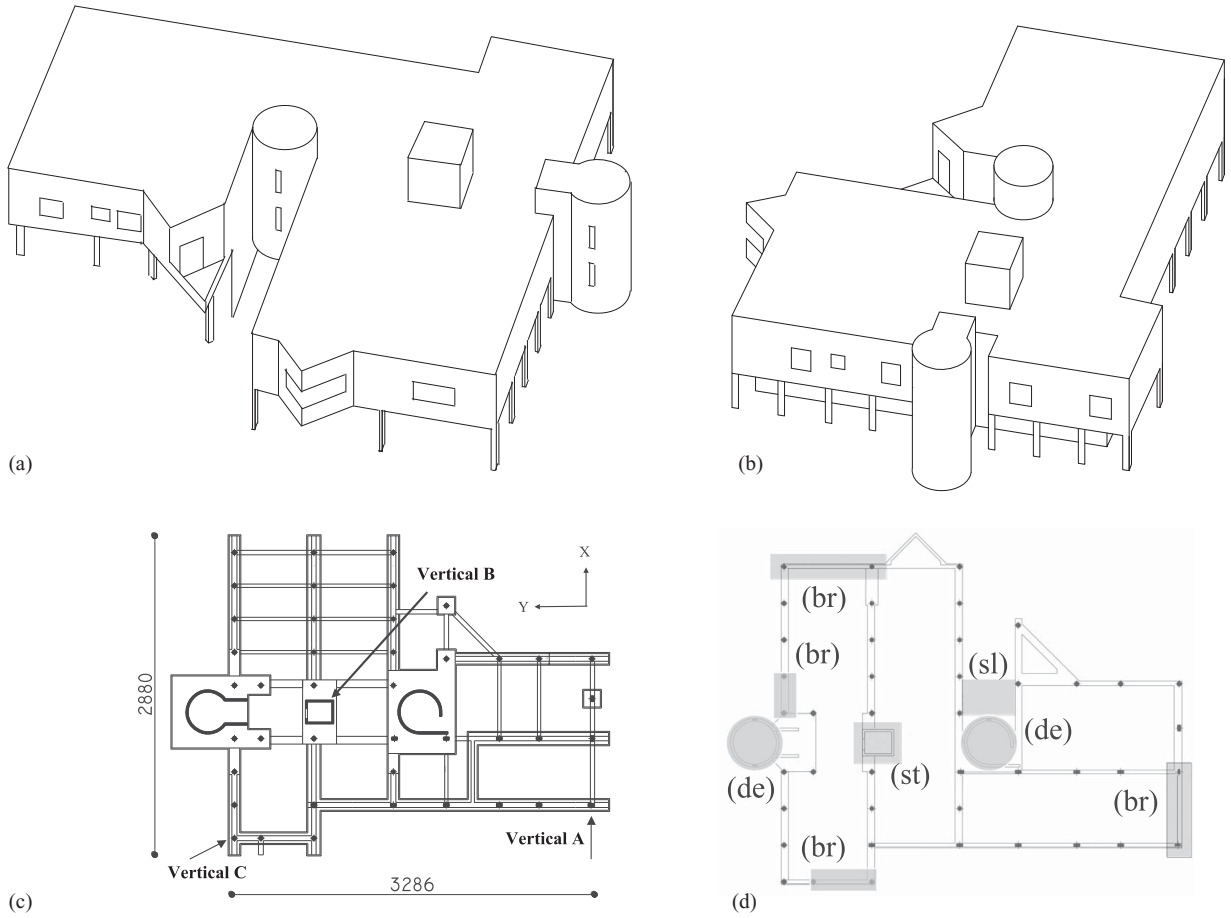

Fig. 2. Abruzzo Regional Fire Service Department, L'Aquila: (a) aerial view from the south; (b) aerial view from the north–east; (c) foundation plan of the building before the retrofit, measures in centimeters, Verticals A, B, and C refer to some alignments relevant for the seismic response; and (d) first-level plan with the locations of the building parts subjected to the interventions: four perimetric frames reinforced with bracings (br), the rectangular hollow-core elevator shaft, reinforced with additional stirrups (st), new slabs (sl), deactivation of the circular shafts to carry only vertical loads (de).

Table 1. Yielding and ultimate chord rotations (%) in the global X direction

	Yielding			Ultimate		
Elements (level)	min	max	mean	min	max	mean
Rectangular columns (1)	0.7	1.1	1.0	1.9	2.8	2.2
Circular columns (1)	0.8	0.9	0.9	1.7	2.1	1.9
Rectangular wall (1)	0.3	0.3	0.3	1.6	1.6	1.6
Columns (2)	0.7	1.0	0.8	2.2	2.8	2.5
Rectangular wall (2)	0.3	0.3	0.3	1.4	1.4	1.4

columns. For the walls, θ_y is 0.3%. At ultimate condition the elements exhibit a minimum chord rotation of 1.4%

Owing to the irregular plan configuration of the building, significant floor torsion effects can be expected. Thus, the approach proposed in Paulay (1997) has been applied to calculate the yielding displacement of each floor. Stiffness reductions for the seismic loads in the X direction [see Fig. 2(c) for the axis convention] of 2.6% at Level 1 and 2.9% at Level 2 are found, whereas in the Y direction the torsional effect is negligible. Knowing the system stiffness at each floor, the relationship between floor shear and interstory displacement, until the yielding of the rectangular hollow-core wall, can be determined. At this point, its stiffness can be set to zero and the subsequent branch is based only on the column stiffness, until the yielding of all elements. Then, the bilinear elastoplastic relationship required by the procedure is obtained by imposing the same energy for the two curves. At this point, the yielding chord rotation of the center of stiffness of each floor $\theta_{y,i}$ can be calculated. The adopted design parameters in the X direction are reported in Table 2.

The yielding displacement of the equivalent SDOF system D_y^* is 29.7 mm. The values of $\theta_{u,i}$, i.e., the ultimate chord rotations at the various floors, must be selected considering the capacities reported in Table 1: selecting 1.1% for both floors, i.e., less than the available minimum of 1.4%, the required ductility μ^* is 1.98. The latter value can be considered acceptable for an existing RC building.

In Fig. 3, the 5% damping displacement response spectrum, as defined in NTC (2018) for the site of the building, is depicted. Owing to the strategic category of the building, a 2,475-year return period spectrum has been adopted for the collapse limit state.

The displacement capacity of the equivalent SDOF system is $M^* D_u^*/L^* = 60.5$ mm. The natural vibration period corresponding to 60.5 mm is 0.456 s, determined from the procedure described in the "Introduction," with $q^* = 1.88$. Consequently, the stiffness of the equivalent SDOF system and the base shear can be calculated and the demand in terms of total shear at each level can be initially obtained applying (19).

The total shear capacity of the existing structure at each level is obtained by summing the shear forces corresponding to the flexural resistance of the vertical elements, considering only the elements with adequate ductile behavior. At Level 1, the shear demand is greater than the shear capacity, thus the difference is carried by

Table 2. Retrofit design in the global X direction

Symbol	unit	Level 1	Level 2	Sum	Overall
H_i	mm	4,200	3,300		
$\theta_{y,i}$	%	0.55	0.43		
$d_{y,i}$	mm	22.3	37.5		
m_i	kN/m/s^2	738	474	1,212	
D_y^*	mm				29.7
M^*	kN/m/s^2				1,212
L^*/M^*	kN/m/s^2				0.97
$\theta_{u,i}$	%	1.1	1.1		
$d_{u,i}$	mm	46.2	82.5		
$d_{u,i}/d_{y,i}$		1.98	2.20		
μ^*					1.98
D_u^*	mm				58.8
q^*					1.88
T^*	s				0.456
K^*	KN/m				230,182
R_y^*	kN				6,842
R_i [Eq. (19)]	kN	3,272	3,380		
$R_i d_{y,i}/D_y^*$	kN	2,570	4,272	6,842	
V_i	kN	6,653	3,380		
$V_{bldg,i}$	kN	3,724	3,592		
$V_{add,i}$	kN	2,929	−212		
α [Eq. (20)]					1
R_i	kN	2,488	3,868		
$R_i d_{y,i}/D_y^*$	kN	1,954	4,888	6,842	
V_i	kN	6,356	3,868		
$V_{add,i}$	kN	2,632	275		
β [Eq. (29)]					4
R_i	kN	1,954	4,200		
$R_i d_{y,i}/D_y^*$	kN	1,535	5,367	6,842	
V_i	kN	6,154	4,200		
$V_{add,i}$	kN	2,430	607		

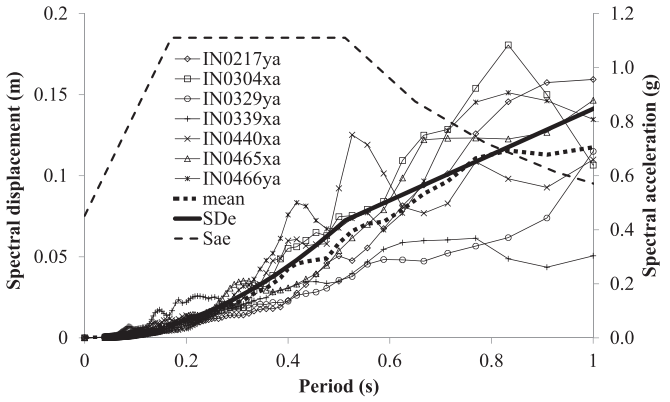

Fig. 3. Design displacement (S_{De}) and acceleration (S_{ae}) response spectra at 5% damping, displacement spectra of the accelerometric records (Table 3), and corresponding mean value.

new additional elements, i.e., new braced frames. At Level 2, the shear demand is smaller than the shear capacity of the existing elements. To cope with this issue, two options have been explored, corresponding to the constraint in Eq. (20) on the overall structural regularity and Eq. (29) on the bracings regularity, respectively.

Following the constraint on the structural regularity, the shear carried by the additional elements at Level 2 is about 10% of the corresponding shear at Level 1, thus an abrupt strength reduction of the bracings is introduced. Following the constraint on the bracings regularity, the previous ratio increases up to 25%. The optimal selection of stiffness and strength distribution at each

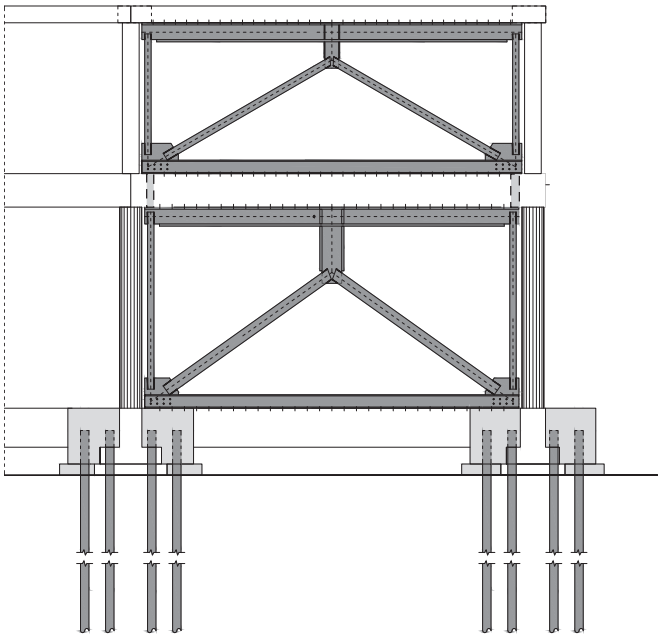

Fig. 4. Front view of a braced frame (new elements are highlighted in dark gray).

level have also been discussed in research devoted to high-rise buildings (Capecchi et al. 1980), leading to results conceptually similar to previous ones.

With the procedure described previously, the total shear carried by the braced frames can be determined, leaving the choice of their number, stiffness, and position to the designer. The knowledge of the flexural stiffness of each vertical element allows us to locate the center of stiffness at each level. The stiffness of the additional bracings was determined in order to maintain the position of the center of stiffness, also in the retrofitted structure. Thus, the previously calculated yielding chord rotations are still valid and can be also attributed to the additional steel braced frames. In the case at hand, two additional braced frames are inserted in each direction, as depicted in Fig. 2(d). The dissipating element of the frame (Fig. 4) consists of the central vertical steel profile, designed to yield at a prescribed horizontal displacement. The other steel elements are designed to carry, in the elastic range, all generated forces, avoiding the transmission of any additional load to the existing joints and members. The foundations of the braced frames have been upgraded to carry the additional loads by additional micropiles.

In order to the check the building performance when the seismic action corresponding to the operational limit state occurs, a simple scaling has been applied to some quantities of Table 1, as already discussed at the end of the previous section. The maximum interstory drift obtained is 0.4%, which can be considered compatible with the strategic function of the building.

Passing on the seismic assessment of the retrofitted configuration, a model has been developed using the OpenSees code (McKenna et al. 2013). The nonlinear behavior of each vertical element has been derived directly from the closed-form calculations and a linearized law between shear force and relative displacement between element joints has been implemented, adopting the OpenSees twoNodeLink element. The bending moment is derived by the code on the basis of the shear-type assumption. Owing to the latter hypothesis, the yielding and ultimate relative displacement between element joints is equal to the product between the corresponding chord rotations and the element length. When the ultimate displacement of the element is achieved, its strength rapidly decreases to

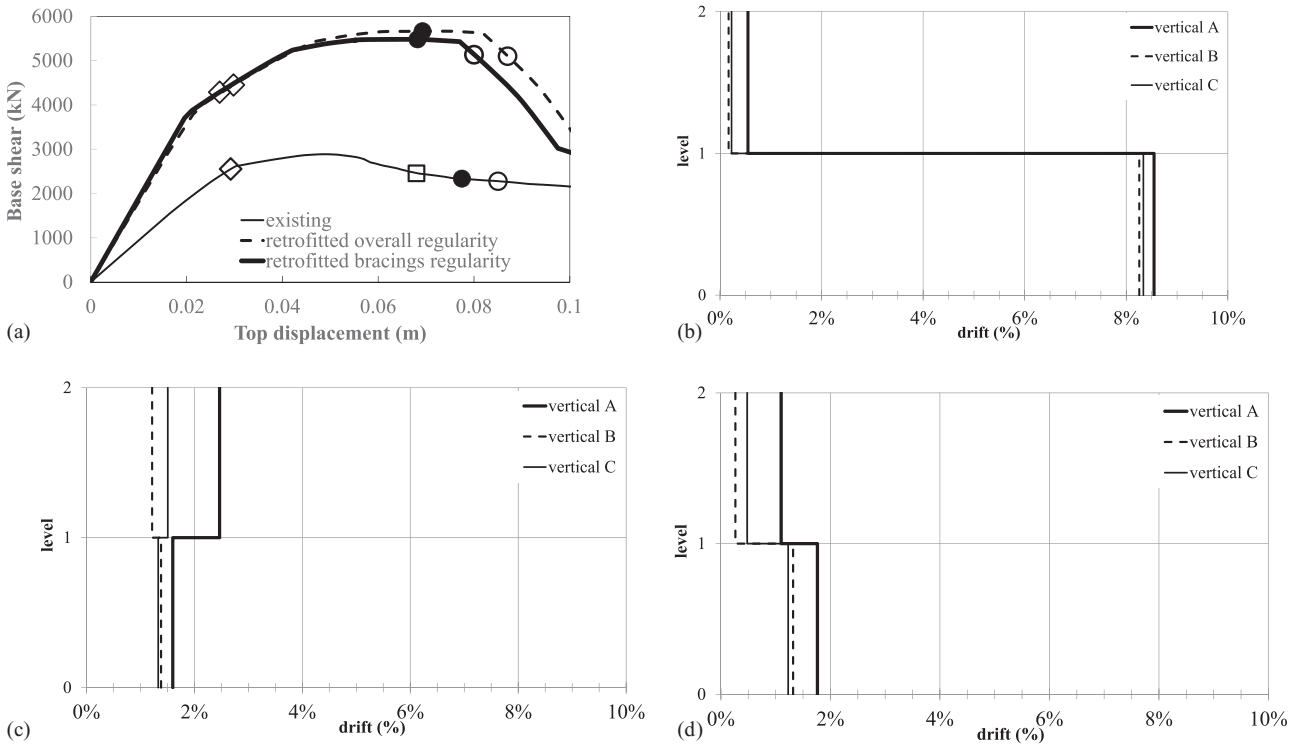

Fig. 5. (a) Nonlinear static analysis, comparison between the existing and the retrofitted structure (overall regularity or bracings regularity criteria); (b) nonlinear dynamic analysis, mean values among seven records of the maximum interstory drifts [the location of the vertical alignments are reported in Fig. 2(c)], existing structure; (c) same analysis for the retrofitted structure designed for the overall vertical regularity; and (d) same analysis for the retrofitted structure designed for the vertical regularity of the additional bracings.

zero. From a numerical point of view, this formulation is very fast and stable. Preliminary comparisons were made between the formulation described previously and fiber models, showing compatible results in a wide deformation range.

Starting from the nonlinear static analyses, Fig. 5(a) shows the pushover curves in the global X direction both for the existing and the retrofitted structures, according to the NTC (2018) procedure. The curves must be read in a comparative perspective, taking into account that the procedure discussed previously leads to different parameters of the substitute SDOF system, with respect to NTC (2018). In the existing structure the circular walls have been considered already deactivated. The diamond symbols correspond to the yielding status in the equivalent bilinear force–displacement law, the white circles to the displacement capacity owing to maximum allowed interstory drifts, the white square to displacement capacity owing to maximum allowed resistance drop, whereas the black circles correspond to the displacement demands. Considering the diamonds and the white circles, the strategy based on both stiffness and strength increments of Fig. 1(b) can be clearly recognized. Furthermore, both the constraints based on overall regularity and bracings regularity are able to satisfy the required seismic performance.

For the comparisons based on nonlinear dynamic analyses, the selection of seven accelerometric records (Fig. 3) compatible with the 5% damping design spectrum was made using the procedure reported in Smerzini and Paolucci (2011). The main parameters of the records are reported in Table 3. For each record the interstory drift on three vertical alignments [the locations are identified as A, B, and C in Fig. 2(c)] was recorded and the maximum values calculated. The mean values among the analyzed records are reported in Fig. 5(b–d), both for the existing and the retrofitted structure. In the existing structure the displacement demands attain very large values at the first floor, incompatible with the collapse limit state performance.

Table 3. Accelerometric records selected for the dynamic analysis

Waveform ID	Earthquake name	Date	Mw	Epicentral distance (km)
465	Erzincan	1992 March 13	6.6	8.97
304	Loma Prieta	1989 October 18	6.9	18.75
217	Olfus	2008 May 29	6.3	8.89
440	Gazli	1976 May 17	6.7	12.78
466	Duzce	1999 November 12	7.1	5.27
329	Darfield	2010 September 03	7.1	9.06
339	Christchurch	2011 February 21	6.2	1.48

For the retrofitted structure designed for the overall vertical regularity, Eq. (20), maximum interstory drifts reach 2.5% at the second level and slightly exceed the vertical members capacities. Instead, when the bracings regularity is pursued, Eq. (29), the interstory drift is well below the element capacities. The analyses have been repeated with a different set of seven records, obtaining similar results. Thus, the observed behavior does not depend on the signal selection. This behavior can be partially related to the linear dynamics of a 2-DOF system, for which the participation coefficient of the second mode, which governs the interstory drift at the upper floor, shows a 13% reduction passing from Eqs. (20)–(29).

It is interesting also to compare the mean value of D_u^*, resulting from the numerical simulations, to the corresponding design value. Thus, Eq. (8) was applied, using the maximum absolute displacement of a point located on the roof near the center of mass. For the solution corresponding to Eq. (20), D_u^* is 65 mm, slightly greater than the design value of about 59 mm. When Eq. (29) is applied, D_u^* is 57 mm, very similar to the design value.

Finally, the design assumption of constant axial forces in the vertical elements was verified: in the element with the maximum variation of about 33% of the axial force, the ultimate moment varies of about 7% and the yielding and ultimate interstory drifts vary by 2% and 2.5%, respectively. Thus, the assumption made at the design phase resulted acceptable.

The discussion reported above has been based on the results of the dynamic analyses with the seismic action applied only in the X direction, thus allowing a better comparison with the design phase and with the results of the pushover analysis. According to several seismic codes, orthogonal effects must be considered and the seismic actions must be applied simultaneously in two horizontal directions. This was checked, repeating the nonlinear dynamic analyses using a set of seven two-component accelerograms. It was observed that the maximum drifts corresponding to the set of single-component records were not exceeded by the two-component results.

Conclusions

When dealing with the rehabilitation of an existing building, several tentative retrofit configurations are usually analyzed until the performance corresponding to the target limit state is achieved; here, a straightforward procedure to determine the retrofitted configuration of the structure directly has been proposed.

First the retrofitted strategies have been discussed, making reference to the use of the nonlinear static analysis procedure widely applied in international seismic codes and standards. Since the retrofitting has been pursued by adding new elements, avoiding strengthening single existing elements, the strategy involving an increase of both strength and stiffness, maintaining unchanged the yielding and ultimate displacements, has been adopted. In particular, the rehabilitation is based only on additional steel bracings.

The displacement-based design, formerly proposed for new buildings, has been extended to existing buildings. Limiting our attention to low-rise reinforced concrete buildings, under the hypotheses of shear-type behavior and constant axial forces in the columns, the yielding chord rotations of the joints have been determined directly and, thus, the deflected shape at yielding has been calculated as well. The yielding displacement of the substitute SDOF system, equivalent to the MDOF system, is easily determined and following a similar approach, based on the ultimate chord rotations, the ultimate displacement of the SDOF system can be calculated. From the displacement design spectrum the characteristics of the retrofitted SDOF system, i.e., vibration period, stiffness, and strength, are determined. Thus, the shear resistances of each floor of the retrofitted MDOF structure can be calculated. The difference between required and available shear resistance has been provided by additional elements, in this case by steel bracings. It is shown that the distribution of shear resistance over the height, furnished by the procedure, is not unique but can be satisfied in different ways, which is resolved by introducing a constraint concerning the vertical regularity. Once the retrofitted configuration is pursued by the direct procedure proposed, this configuration has been checked with the seismic assessment analyses specified by the code.

The proposed procedure has been applied to a case study, corresponding to a real retrofit project of a strategic building, ascertaining in detail the applicability of the various steps described and also confirming the suitability of the assumptions introduced. The retrofitted configurations, obtained by applying two different regularity constraints on the shear resistances of floors, substantially satisfy in both cases the code requirements, confirming the effectiveness of the procedure, along with its assumptions and the adopted strategy involving both stiffness and strength increments.

The nonlinear dynamic analyses, developed with a significant set of natural accelerograms, suitably scaled to meet a target spectrum, provided further insight into the seismic behavior of the retrofitted structure, that cannot be evidenced by static analyses. The effectiveness of retrofitting has again been confirmed. Not surprisingly, it was found that the vertical regularity significantly affects the seismic performance and, specifically, one version of the constraint is more effective than the other. Moreover, the numerical results make it possible to verify the feasibility of the assumptions referred to in the procedure.

Acknowledgments

This work has been partially supported by the MIUR (Ministry of Education, University and Research) under the Project PRIN 2015-2018, P.I. Fabrizio Vestroni, "Identification and Monitoring of Complex Structural Systems."

Disclaimer

The views and conclusions contained here are those of the authors, and should not be interpreted as necessarily representing official policies, either expressed or implied, of the Italian Government.

References

ASCE. 2013. *Seismic rehabilitation of existing buildings*. ASCE-41. Reston, VA: Structural Engineering Institute, ASCE.

ATC (Applied Technology Council). 1996. *Seismic evaluation and retrofit of concrete buildings*. ATC-40. Redwood City, CA: ATC.

Barbagallo, F., M. Bosco, A. Ghersi, E. Marino, and P. Rossi. 2018. "Seismic retrofitting of eccentrically braced frames by rocking walls and viscous dampers." *Key. Eng. Mater.* 763: 1105–1112.

Cáelebi, M., et al. 2010. "Recorded motions of the 6 April 2009 Mw 6.3 L'Aquila, Italy, earthquake and implications for building structural damage: Overview." *Earthq. Spectra* 26 (3): 651–684.

Capecchi, D., G. Rega, and F. Vestroni. 1980. "A study of the effect of stiffness distribution on nonlinear seismic response of multi-degree-of-freedom structures." *Eng. Struct.* 2 (4): 244–252.

Chopra, A., and R. Goel. 2001. "Direct displacement-based design: Use of inelastic vs. Elastic design spectra." *Earthq. Spectra* 17 (1): 47–64.

EN (European Standard). 2004. *Eurocode 8: Design of structures for earthquake resistance—Part 1: General rules, seismic actions and rules for buildings*. EN 1998-1. Bruxelles: European Committee for Standardization.

EN (European Standard). 2005. *Eurocode 8: Design of structures for earthquake resistance—Part 3: Assessment and retrofitting of buildings*. EN 1998-3. Bruxelles: European Committee for Standardization.

Fajfar, P. 1999. "Capacity spectrum method based on inelastic demand spectra." *Earthquake Eng. Struct. Dyn.* 28: 979–993.

Fajfar, P., and P. Gašperšič. 1996. "The N2 method for the seismic damage analysis of RC buildings." *Earthquake Eng. Struct. Dyn.* 25 (1): 31–46.

FEMA (Federal Emergency Management Agency). 2005. *Improvement of nonlinear static seismic analysis procedures*. FEMA-440. Washington, DC: FEMA.

Grande, E., and A. Rasulo. 2013. "Seismic assessment of concentric X-braced steel frames." *Eng. Struct.* 49: 983–995.

Grande, E., and A. Rasulo. 2015. "A simple approach for seismic retrofit of low-rise concentric X-braced steel frames." *J. Constr. Steel Res.* 107: 162–172.

Kim, J., and H. Choi. 2006. "Displacement-based design of supplemental dampers for seismic retrofit of a framed structure." *J. Struct. Eng.* 132 (6): 873–883.

Lin, Y.-Y., K.-C. Chang, and C.-Y. Chen. 2008. "Direct displacement-based design for seismic retrofit of existing buildings using nonlinear viscous dampers." *Bull. Earthquake Eng.* 6 (3): 535–552.

McKenna, F., et al. 2013. *Open system for earthquake engineering simulation (OpenSees) rel. 2.4.0*. Berkeley, CA: Pacific Earthquake Engineering Research Center.

Medhekar, M., and D. Kennedy. 2000. "Displacement-based seismic design of buildings—Theory." *Eng. Struct.* 22 (3): 201–209.

Miranda, E., and J. Ruiz-Garcia. 2002. "Evaluation of approximate methods to estimate maximum inelastic displacement demands." *Earthquake Eng. Struct. Dyn.* 31 (3): 539–560.

Moehle, J. 1992. "Displacement-based design of RC structures subjected to earthquakes." *Earthq. Spectra* 8 (3): 403–428.

NTC (Norme Tecniche per le Costruzioni, Building Code). 2018. *Decree of 2018 January 17th.* [In Italian.] Rome: Ministry of Infrastuctures and Transport.

Nuzzo, I., D. Losanno, and N. Caterino. 2019. "Seismic design and retrofit of frame structures with hysteretic dampers: a simplified displacement-based procedure." *Bull. Earthquake Eng.* 17 (5): 2787–2819.

Panagiotakos, T., and M. Fardis. 2001. "A displacement-based seismic design procedure for RC buildings and comparison with EC8." *Earthquake Eng. Struct. Dyn.* 30 (10): 1439–1462.

Paulay, T. 1997. "Displacement-based design approach to earthquake-induced torsion in ductile buildings." *Eng. Struct.* 19 (9): 699–707.

Price, H., A. De Sortis, and M. Schotanus. 2012. "Performance of the San Salvatore regional hospital in the 2009 L'Aquila earthquake." *Earthq. Spectra* 28 (1): 239–256.

Priestley, M. 1993. "Myths and fallacies in earthquake engineering - conflicts between design and reality." *Bull. N. Z. Soc. Earthqu. Eng.* 26 (3): 329–341.

Priestley, M. J. N. 1997. "Displacement-based seismic assessment of reinforced concrete buildings." *J. Earthquake Eng.* 1 (1): 157–192.

Qi, X., and J. Moehle. 1991. *Displacement design approach for reinforced concrete structures subjected to earthquakes*. Report No. UCB/EERC-91.2. Berkeley, CA: Earthquake Engineering Research Center, University of California.

Rossi, P. P. 2007. "A design procedure for tied braced frames." *Earthquake Eng. Strct. Dyn.* 36 (14): 2227–2248.

Smerzini, C., and R. Paolucci. 2011. *SIMBAD: A database with selected input motions for displacement-based assessment and design*. Rep. No. DPC-ReLUIS 2010–2013 project. Milan, Italy: Dept. of Structural Engineering, Politecnico di Milano.

Sullivan, T., G. Calvi, M. Priestley, and M. Kowalsky. 2003. "The limitations and performances of different displacement based design methods." *J. Earthquake Eng.* 7 (SPEC. 1): 201–241.

Sun, T., Y. Kurama, and J. Ou. 2018. "Practical displacement-based seismic design approach for PWF structures with supplemental yielding dissipators." *Eng. Struct.* 172: 538–553.

Thermou, G., S. Pantazopoulou, and A. Elnashai. 2007. "Design methodology for seismic upgrading of substandard reinforced concrete structures." *J. Earthquake Eng.* 11 (4): 582–606.

Thermou, G., and M. Psaltakis. 2018. "Retrofit design methodology for substandard R.C. buildings with torsional sensitivity." *J. Earthquake Eng.* 22 (7): 1233–1258.

Vidot-Vega, A., and M. Kowalsky. 2013. "Drift, strain limits and ductility demands for RC moment frames designed with displacement-based and force-based design methods." *Eng. Struct.* 51: 128–140.